Electronic Supplementary Information

Excellent catalytic properties of luminescent Cu@Cu_2S nanozymes and antibacterial application

Yuezhen He,*[a] Manyue Yin, [a] Jian Sun, [a] Jie Chen, [b] Kuimin Jiao, [a] Jiantao Wen, [a] Yan Chen, [a] Baojuan Wang, *[b] Feng Gao, [a] and Lun Wang, [a]

a. College of Chemistry and Materials Science, Anhui Normal University, Key Laboratory of Functional Molecular Solids, Ministry of Education, Anhui Laboratory of Molecular-Based Materials, Anhui Key Laboratory of Chemo-Biosensing, Wuhu 241002, China

b. College of Life Sciences, Anhui Normal University, Anhui Provincial Key Laboratory of Molecular Enzymology and Mechanism of Major Diseases and Key Laboratory of Biomedicine in Gene Diseases and Health of Anhui Higher Education Institutes, Wuhu 241000, China

1 Experimental sectiom

Chemicals and Apparatus: L-ascorbic acid (AA), glutathione (GSH, Reduced) and Copper chloride were brought from Aladdin chemistry Co. Ltd (Shanghai, China). Other reagents were purchased from Sinopharm Chemical Reagent Co. Ltd (Shanghai, China). All the other reagents were analytical reagent grade and were used without further purification. Ultrapure water purified with a Millipore system (18.2 MΩ) was used throughout the experiments.

The morphology of Cu_2O@CuO and Cu@Cu_2S nanozymes were recorded with a HT-7700 transmission electron microscope (Hitachi, Japan). High-resolution transmission electron microscope (HRTEM) were captured by using a Tecnai G220S-TWIN transmission electron microscope (FEI, USA). The fluorescence spectra were obtained by a Lumina Fluorescence Spectrometer (Thermo Fisher Scientific, Korea). UV−vis absorption spectra were carried out on a Hitachi UV-2910 spectrophotometer (Hitachi, Japan).

Synthesis of Cu_2O@CuO nanozymes: 0.6 mmol of NaOH and 0.6 mmol of AA were dissolved in 50 mL of water to form a clear solution. 10 mL of the mixture was added dropwise

into 15 mL of $CuCl_2$ aqueous solution (0.025mM) under srirring to form Cu_2O@CuO nanoparticles. With the aid of AA, the CuO nanoparticles were spontaneously formed in the chemical precipitation process, and parts of CuO were reduced to Cu_2O by excess AA. The preparation of Cu_2O@CuO in the chemical precipitation was detailed in Eq S1.

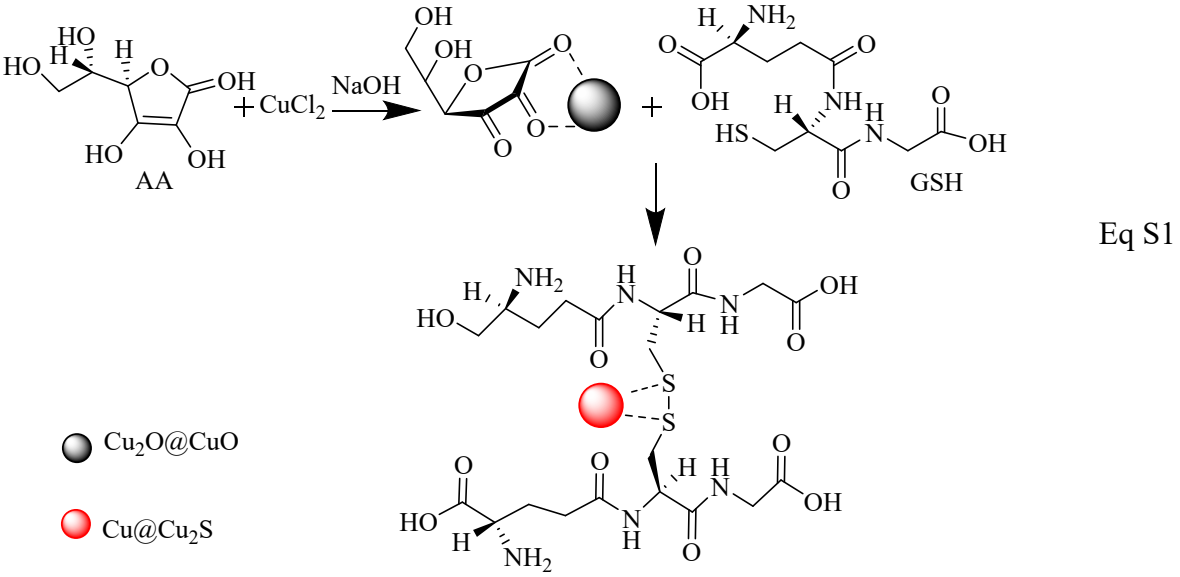

Eq S1

Synthesis of Cu@Cu_2S nanozymes: The aqueous solution of GSH (20 mL, 40 mM) was mixed with the as prepared Cu_2O@CuO nanoparticles (3.5 mL), and stirring for 20 min at room temperature, until white precipitation was generated. The obtained Cu@Cu_2S nanozymes were collected by centrifugation at 8000 rpm for 10 min, and washed with ethanol three times. The product was dispersed again into the water and stored at 4 °C for further use. The Cu_2S nanoparticles were prepared from Cu_2O@CuO nanoparticles in the ligand exchange process due to the stronger affinity of Cu–S than of Cu–O, and only a tiny amount of Cu_2S nanoparticles were reduced to Cu nanoparticles by GSH. Only a tiny amount of Cu_2S nanoparticles were reduced to Cu nanoparticles by GSH. The preparation of Cu@Cu_2S in the ligand exchange process was detailed in Eq S1.

Oxidase-like of two Cu-base nanozymes: The oxidase-like activity of the Cu_2O@CuO nanozymes and Cu@Cu_2S nanozymes was evaluated by using *p*-terephthalic acid (*p*TA) as a substrates. *p*TA (50 mM) was dissolved in NaOH aqueous solution (1 M). The Cu_2O@CuO nanodots (0.5 mM) or Cu@Cu_2S nanodots (0.5 mM) were added to the *p*TA solutions (0.5 mM). After mixing for 30 min, the fluorescent spectrums were detected under 312 nm wavelength excitation.

Peroxidase-like activity of two Cu-base nanozymes: The peroxidase-like activity of the Cu_2O@CuO nanozymes and Cu@Cu_2S nanozymes was evaluated by using the oxidation of *p*TA and degradation of methylene blue (MB) in the presence of H_2O_2. For *p*TA oxidation, *p*TA (0.5 mM), H_2O_2 (1 mM), and Cu_2O@CuO nanodots (0.5 mM) or Cu@Cu_2S nanodots (0.5 mM) were mixed in the 25 mM phosphate buffer solutions (pH 5.0). After mixing for 10 min, the fluorescent spectrums were detected under 312 nm wavelength excitation. For MB degradation, MB (10 μg mL^{-1}), H_2O_2 (1 mM), and Cu_2O@CuO nanodots (0.5 mM) or Cu@Cu_2S nanodots (0.5 mM) were mixed in the 25 mM phosphate buffer solutions (pH 7.4). ·OH-induced MB degradation was measured by UV-vis absorption spectrum in the range of 500 nm to 800 nm.

Minimum inhibitory concentration: *Staphylococcus aureus* (*S. aureus*) and *Escherichia coli* (*E. coli*) were chosen as the representatives of Gram-positive and Gram-negative bacteria in the test. The bacteriun were cultured at 37 °C and 180 rpm in 5 mL of Luria–Bertani (LB) liquid medium until the OD_{600} reached 0.6. First, we test the antibacterial activity of Cu_2O@CuO and Cu@Cu_2S nanozymes, the results (Fig. S15) showed that the antibacterial activity of Cu@Cu_2S nanozymes was much stronger than that of Cu_2O@CuO nanozymes, so we focused on Cu@Cu_2S nanozymes in following experiment.

Various concentrations of Cu@Cu_2S nanozymes (0, 0.46, 0.94, 1.88, 3.75, 7.5, 15.0, 30.0 and 60.0 μg mL^{-1}) were seperately added to the bacterium with continuous shaking at 180 rpm, then growth of organisms was observed by measuring OD at 600 nm until 24 h.

Bacterial growth curves test: The growth curves of the bacterium (including *S. aureus and E. coli*) were determined by consecutive double dilution method with different doses of Cu@Cu_2S nanozymes (0, 0.46, 0.94, 1.88, 3.75, 7.5, 15.0, 30.0 and 60.0 μg mL^{-1}). At first, the concentration of bacterium were adjusted to 0.6 of OD_{600}. The different doses of Cu@Cu_2S nanozymes were added to the bacteria with continuous shaking at 180 rpm, then growth of organisms was observed by measuring OD at 600 nm every two hours until 24 h.

Inhibition zone test: The antibacterial performance of Cu@Cu_2S nanozymes was assessed by inhibition zone method. The bacterium were cultured until whose optical density (OD_{600}) reached 0.6. Then, 100 μL of the bacterial suspension was uniformly spreaded to sterile LB agar plates. Subsequently, 200 μL various concentrations of Cu@Cu_2S nanozymes (0.25, 0.50, 1.0 mg mL^{-1}), and PBS buffer were separately added to four sterilized Oxford cup, and the plate was incubated at 37 °C. The inhibition diameters of the zone were detected after incubation for 24 h. The experiment of Oxford cup was repeated three times independently.

Bacterial imaging with Cu@Cu_2S **nanozymes:** *S. aureus* or *E. coli* solution (OD_{600} = 0.6) were cultured in 1 mL LB liquid medium with 10 mg mL^{-1} Cu@Cu_2S nanozymes for 2.5 h at 37 °C and 180 rpm. The bacterium were seperately collected by centrifugation at 8000 rpm for 5 min and re-dispersed in 1mL of PBS buffer solution (pH=7.4). Fluorescent images were taken using an upright fluorescence microscope Axio Image A2 (Zeiss, Germany).

Morphological observation for bacterium by SEM: The bacterium (*S. aureus* and *E. coli*) were severally incubated in LB liquid medium with Cu@Cu_2S nanozymes (60.0 μg mL^{-1}) for

4 h, while the control group was treated without Cu@Cu_2S nanozymes. The bacteria was collected by 8000 rpm centrifugation for 10 min, and cleared by PBS buffer for three times. Next, we added 2.5% glutaraldehyde to fix the bacteria for 30 min. Then the bacteria was dehydrated with gradient ethanol. Finally, it was transferred to the clean silicon slice to dry by vacuum and sputter-coated with gold before observed by SEM.

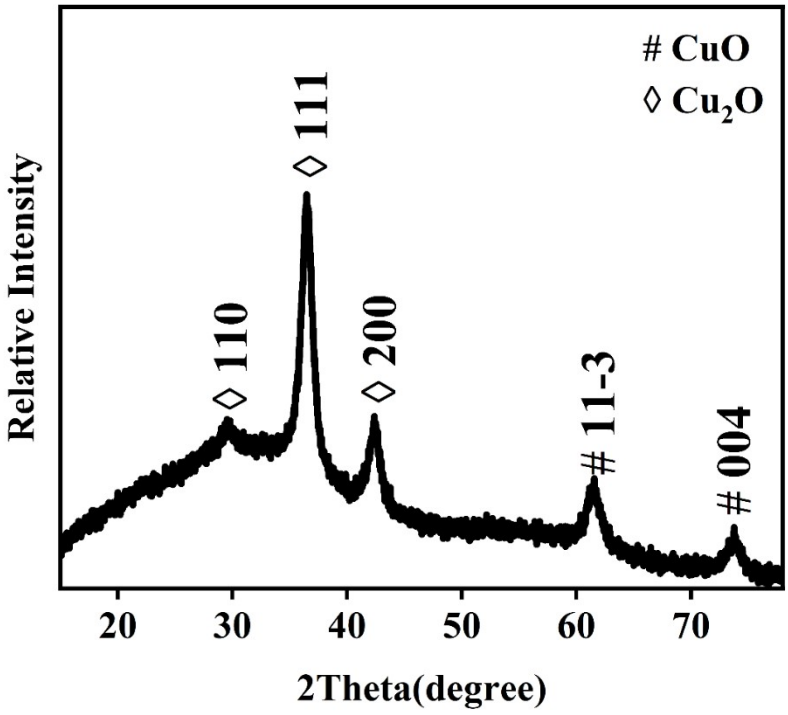

Fig. S1 XRD patterns of Cu_2O@CuO nanozymes. The main characteristic diffraction peaks of Cu_2O@CuO nanozymes at 29.6°, 36.4°, and 42.3°agreed well with the (110), (111), and (200) reflections of Cu_2O (JCPDS no. 05-0667), which indicated that the nanozymes contained of Cu_2O. Moreover, two XRD peaks located at 61.3°, and 73.5° were indexed to (11-3) and (004) reflections of CuO (JCPDS no. 48-1548), which indicated that the nanozymes included CuO.

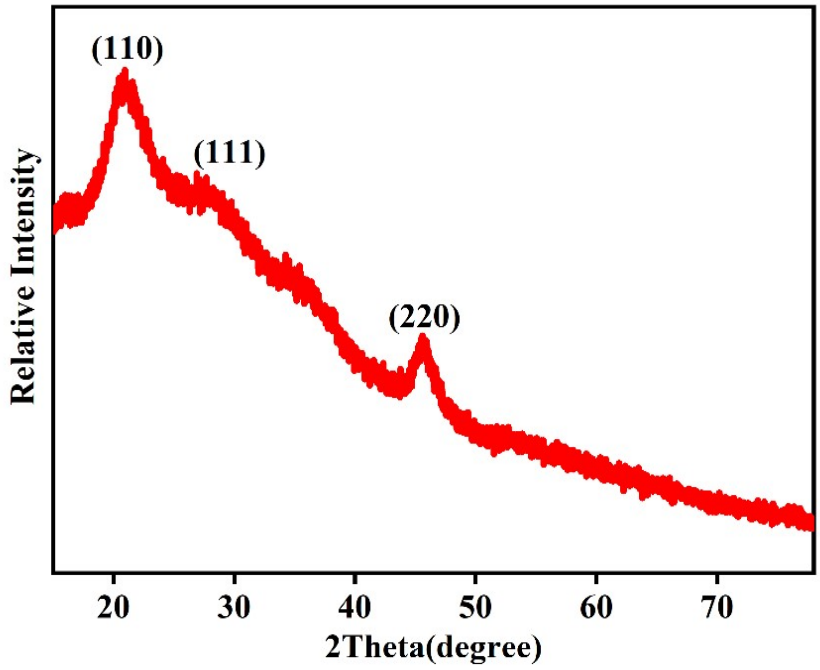

Fig. S2 XRD patterns of Cu@Cu_2S nanozymes. The XRD peaks at 22.6°, 27.8° and 46.1° of Cu@Cu_2S nanozymes were indexed to the (110), (111) and (220) of the face-centered cubic

(fcc) form of Cu_2S (JCPDS no. 53-0522), which illustrated that the nanozymes composed mainly of Cu_2S.

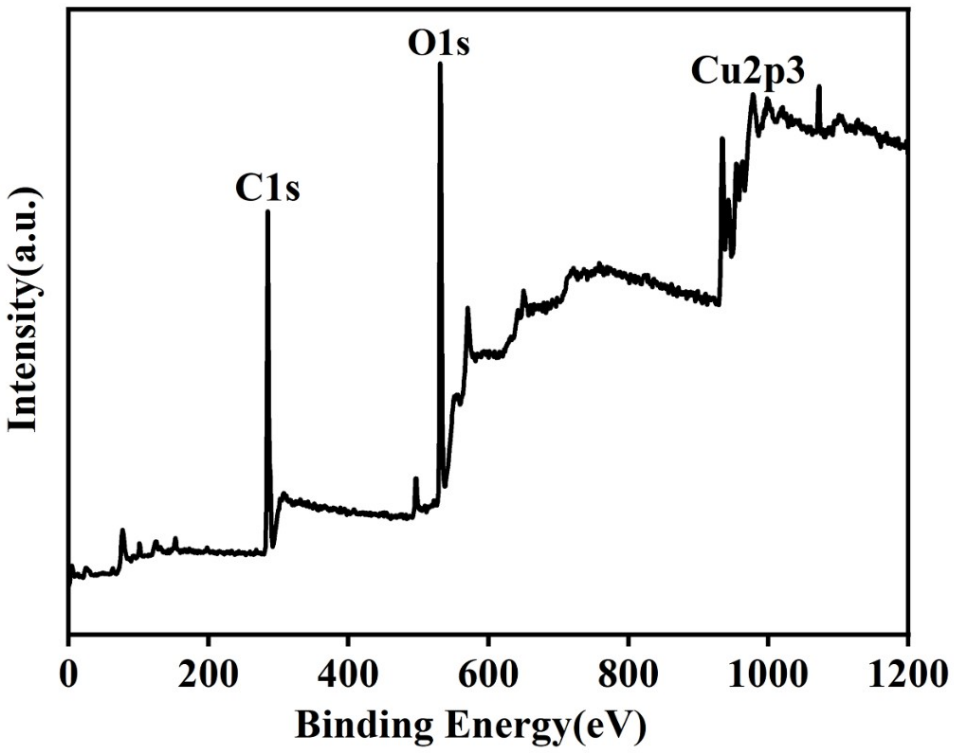

Fig. S3 XPS spectrum of Cu_2O@CuO nanozymes

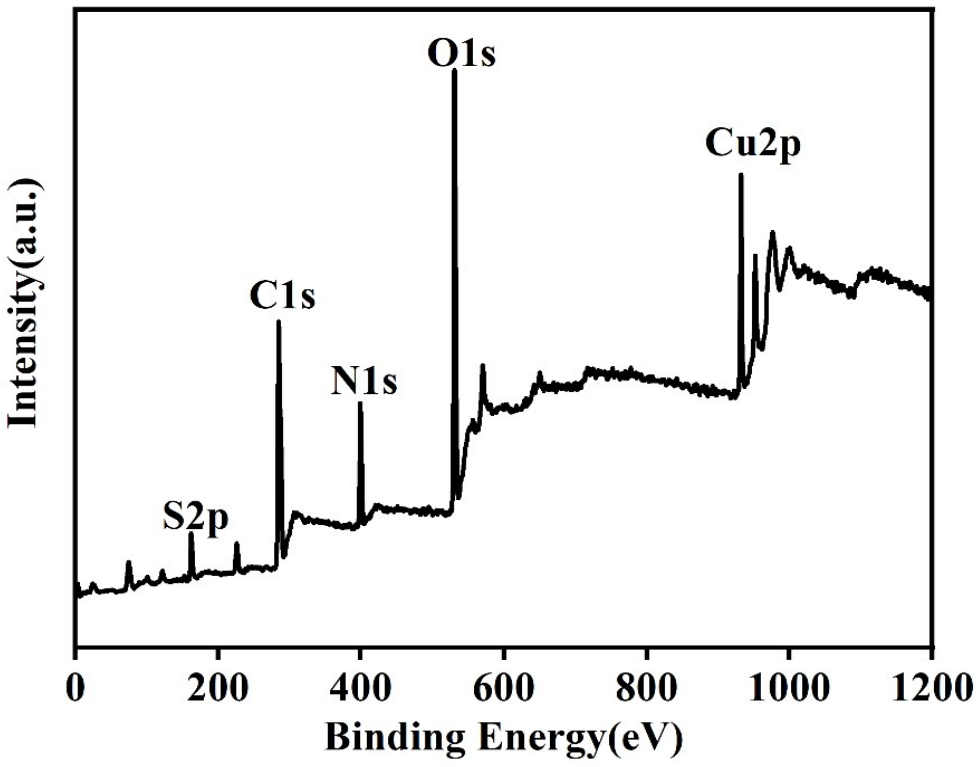

Fig. S4 XPS spectrum of Cu@Cu_2S nanozymes

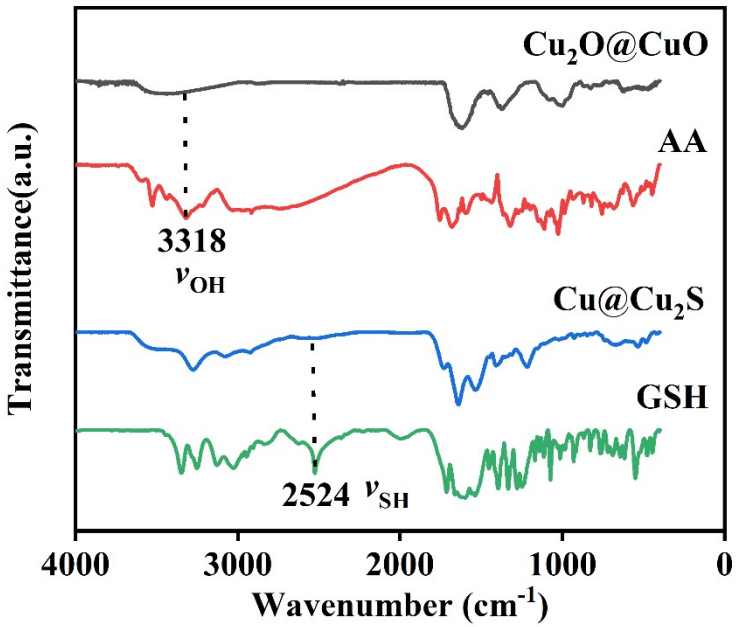

Fig. S5 FTIR spectra of Cu_2O@CuO nanozymes, AA, Cu@Cu_2S nanozymes, and GSH. Some functional groups of AA were found on the surface of the Cu_2O@CuO nanozymes, and the vibration intensity of O–H bone at 3318 cm^{-1} disappeared, verifying that AA molecules bind onto the Cu_2O@CuO nanozymes through Cu–O bonds. For Cu@Cu_2S nanozymes, the vibration intensity of S–H bone at 2524 cm^{-1} disappeared, which could be attributed to the GSH anchoring at the nanomaterial surface through Cu–S bonding.

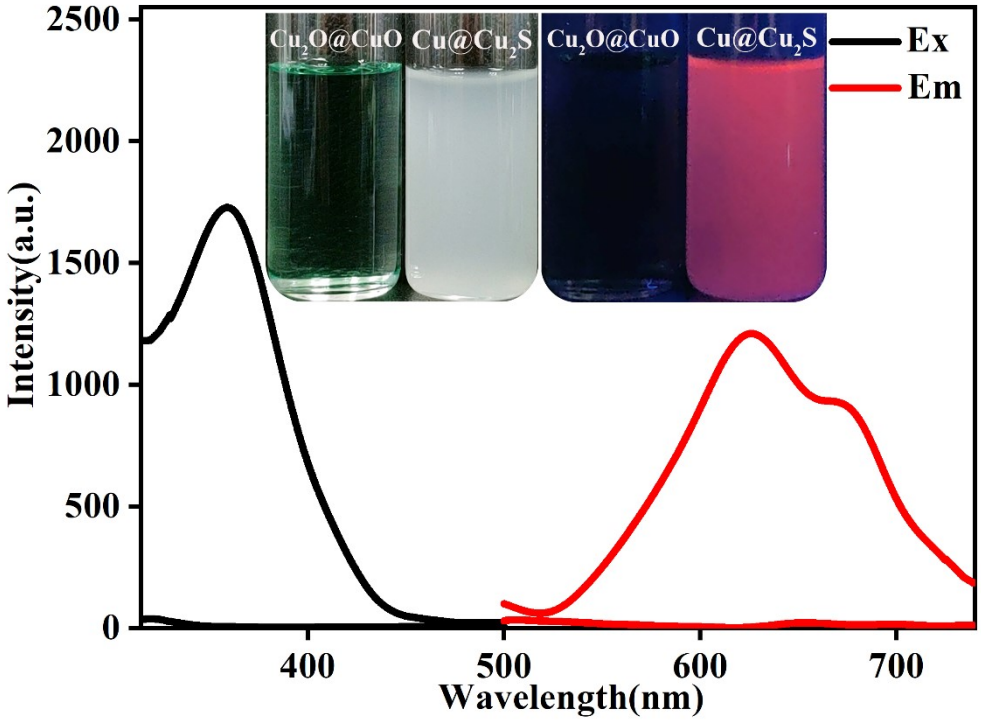

Fig. S6 Excitation and emission spectra of Cu_2O@CuO and Cu@Cu_2S, Inset: Photo of Cu_2O@CuO and Cu@Cu_2S (right), and their fluorescent photo under 365-nm UV light

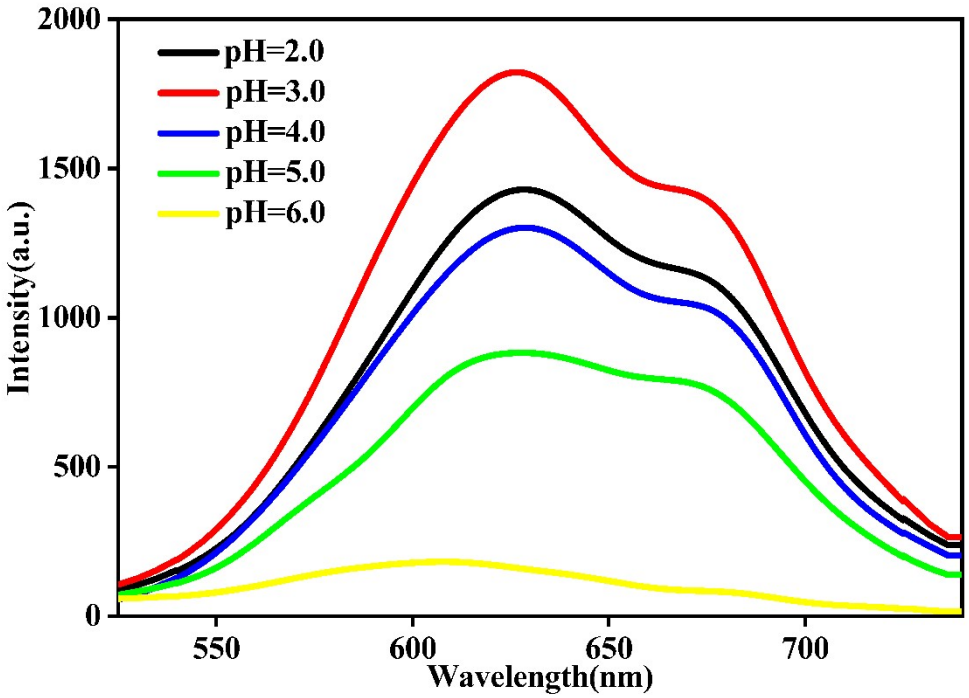

Fig. S7 Luminescence spectra of Cu@Cu_2S aggregates at different pH values. The Cu@Cu_2S exhibit a pH-responsive emission, the fluorescence intensity increased significantly with the pH decreased from 6.0 to 3.0. These indicate that a variation in the pH of an aqueous solution changes the structure of Cu@Cu_2S from monodispersed states to aggregates.

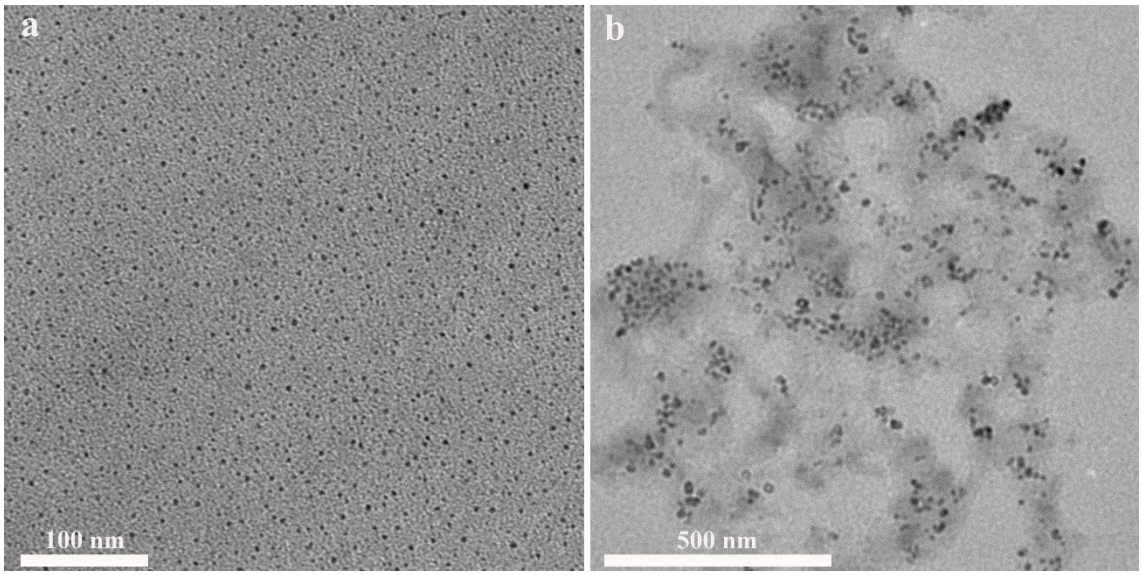

Fig. S8 TEM image of Cu@Cu_2S nanozymes at: a) pH 6.0, and b) pH 3.0. The aggregates of nanozymes at pH 3.0 are more than that at pH 6.0. Therefore, it is reasonable to believe that the as-prepared Cu@Cu_2S have a pH-responsive aggregation-induced emission.

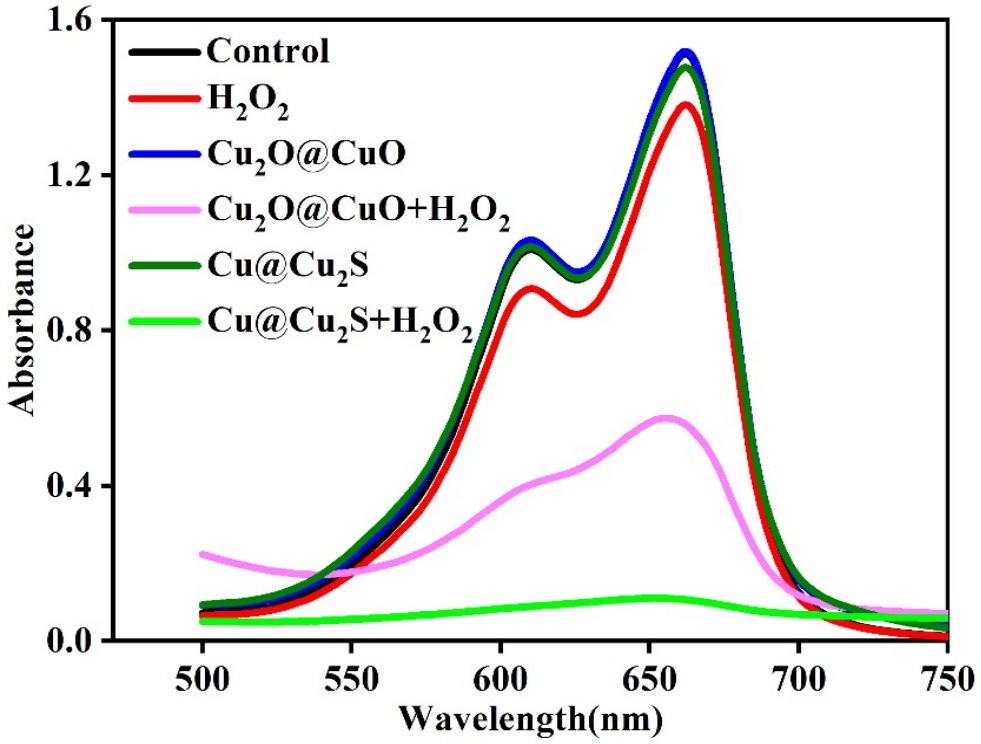

Fig. S9 Peroxidase-like activity of Cu_2O@CuO and Cu@Cu_2S with MB degradation

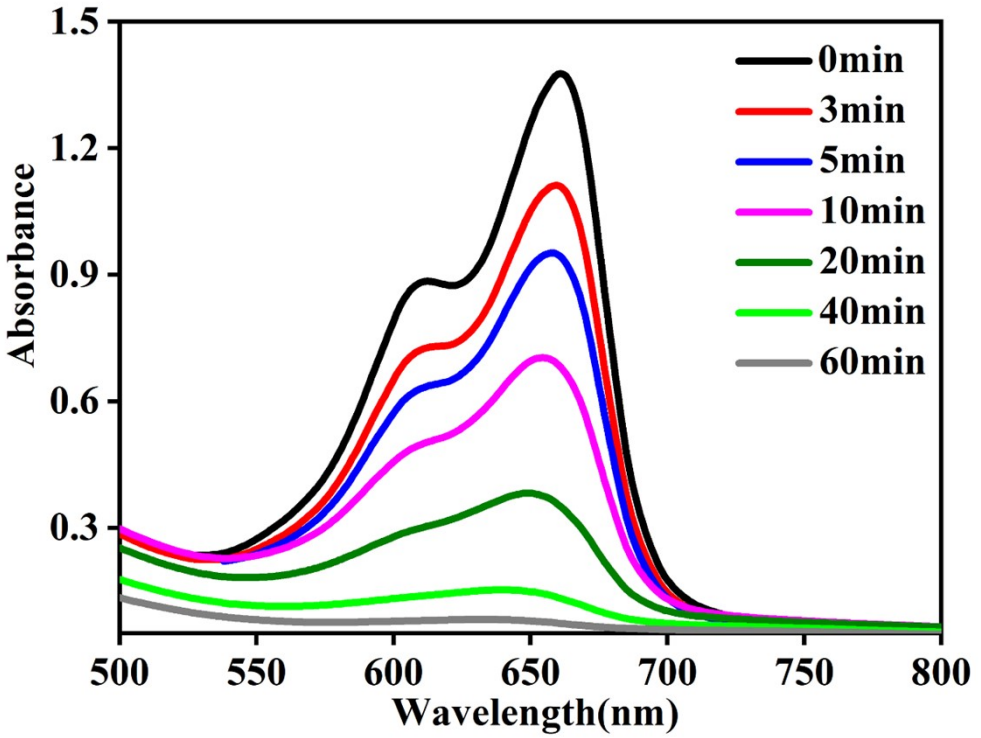

Fig. S10 Degradation process of MB in the presence of Cu_2O@CuO and H_2O_2

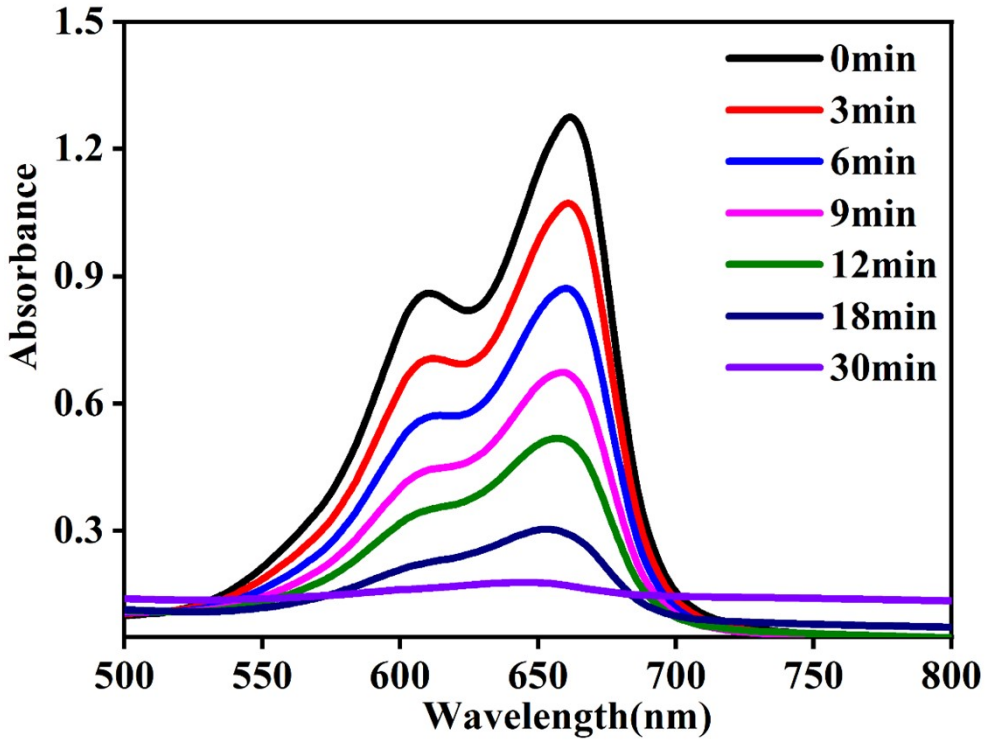

Fig. S11 Degradation process of MB in the presence of $Cu@Cu_2S$ and H_2O_2

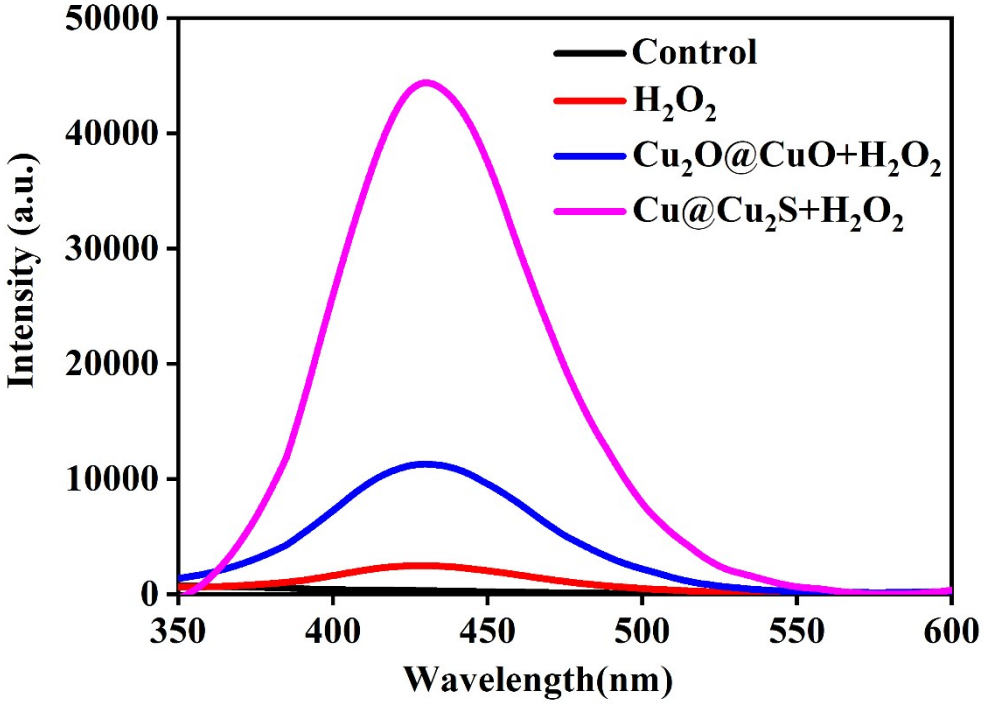

Fig. S12 Peroxidase-like activity of $Cu_2O@CuO$ and $Cu@Cu_2S$ with *p*TA oxidation and H_2O_2

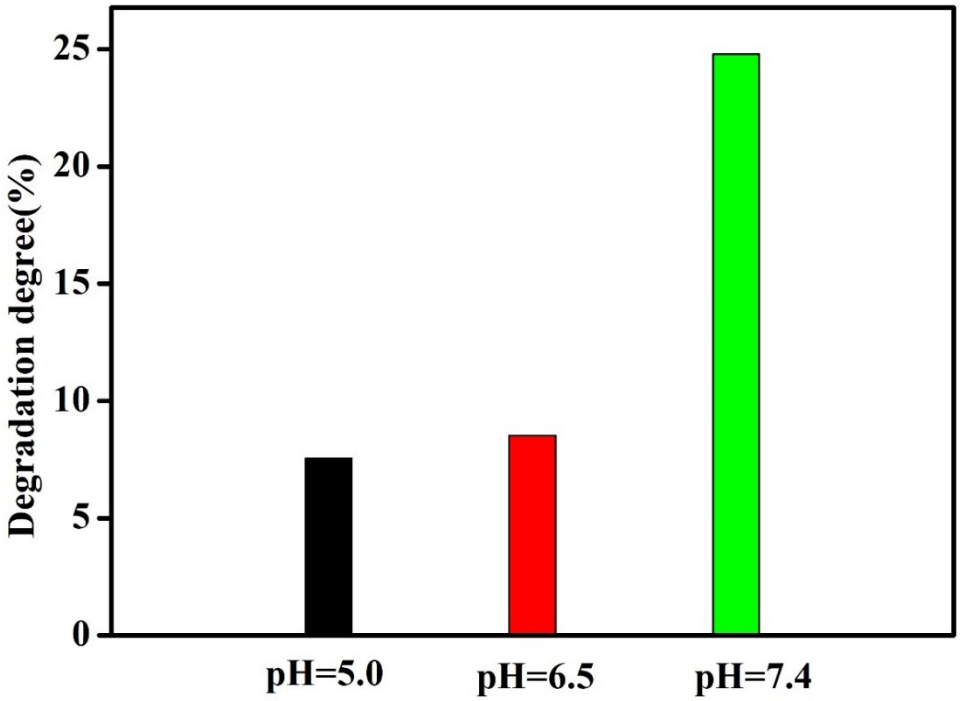

Fig. S13 MB degradation at different pH conditions in the presence of Cu_2O@CuO and H_2O_2. The reaction speed of MB degradation increased with increasing of pH values, and the rate in pH 7.4 raised by 26.8% over that in pH 5.0.

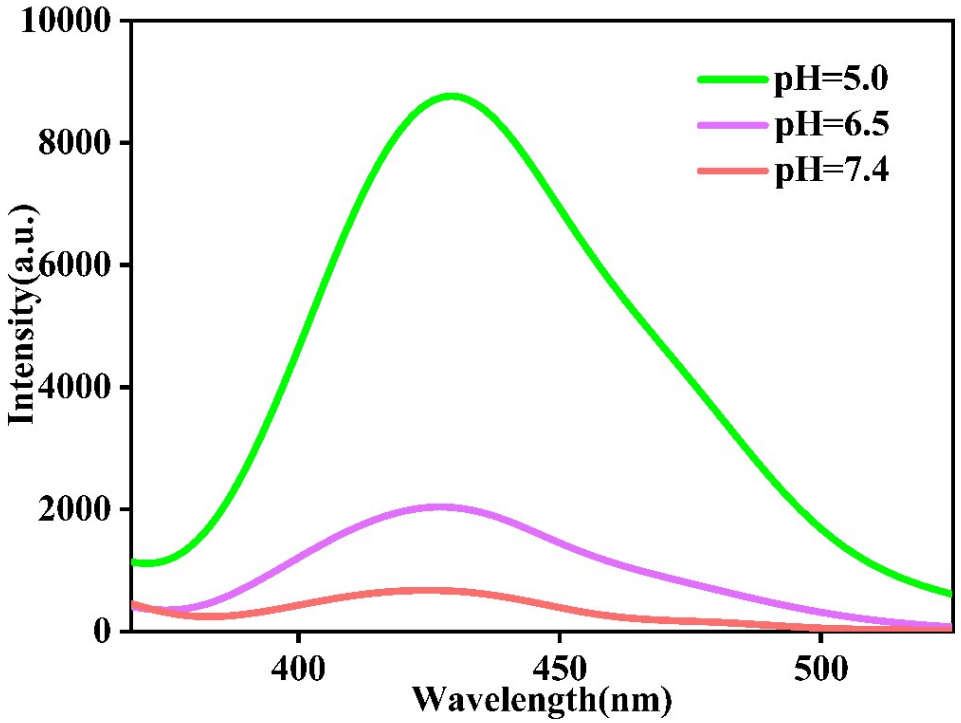

Fig. S14 Fluorescent spectra of *p*TA oxidation at different pH conditions in the presence of Cu_2O@CuO and H_2O_2. The oxidation of *p*TA had dramatically declined with the increase of pH values, and the rate in pH 7.4 was only a tenth of the speed in pH 5.0.

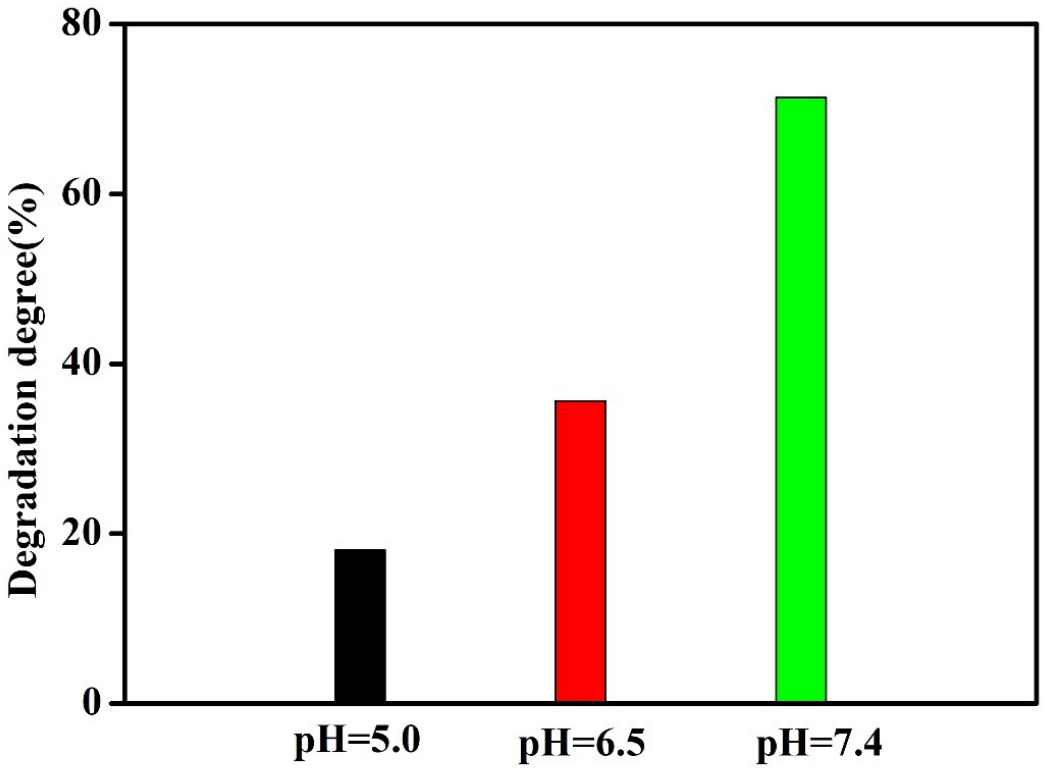

Fig. S15 MB degradation at different pH conditions in the presence of Cu@Cu_2S and H_2O_2. The reaction rates of MB degradation also increased with the increasing of pH values, and the rate in pH 7.4 raised four times as compared to that in pH 5.

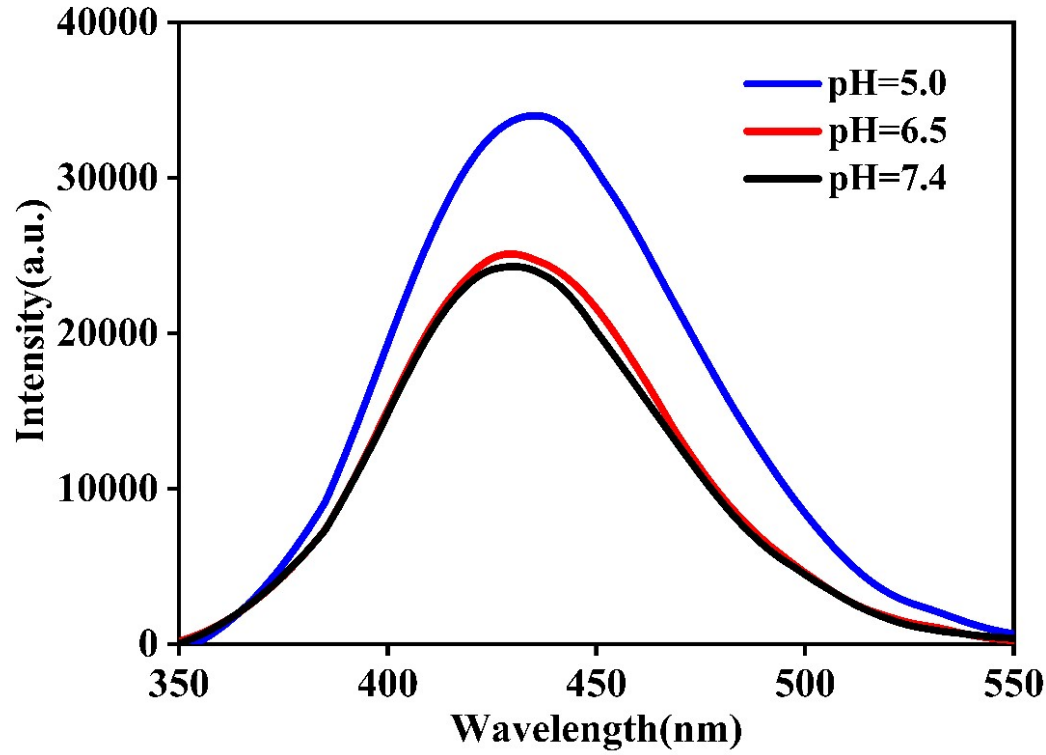

Fig. S16 Fluorescent spectra of *p*TA oxidation at different pH conditions in the presence of Cu@Cu_2S and H_2O_2. *p*TA oxidation in pH 7.4 remained at 73% of the rates in pH 5.0.

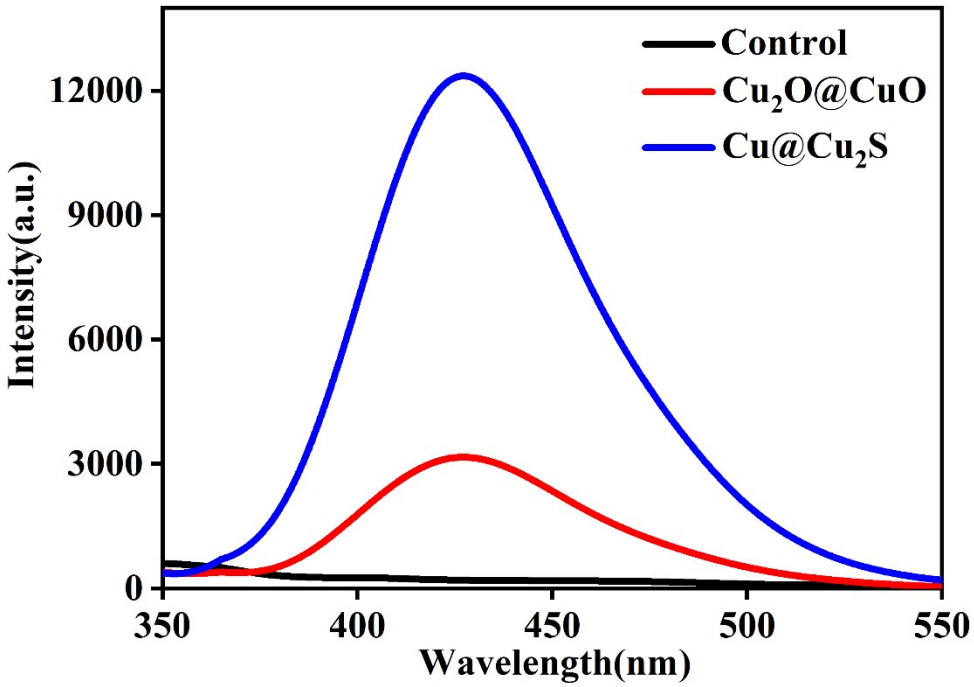

Fig. S17 oxidase-like activity of Cu_2O@CuO and Cu@Cu_2S with *p*TA oxidation.

Fig. S18 Turbidity changes of *S. aureus* with Cu_2O@CuO, Cu@Cu_2S and antibiotics in test tubes: 2: Contral; 3: Antibiotics; 4, 5: Cu_2O@CuO; 6, 7: Cu@Cu_2S

Table S1 OD_{600} values of the above-mentioned *S. aureus'* turbidity

Sample	Control	Antibiotics	Cu_2O@CuO		Cu@Cu_2S	
OD_{600}	2.029	0.016	0.291	0.796	0.007	0.009

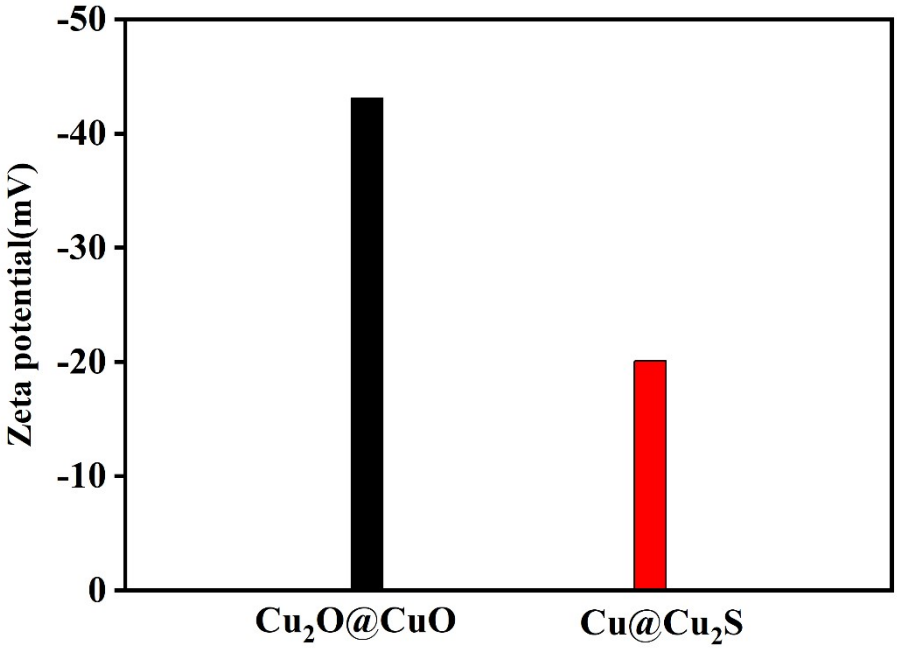

Fig. S19 Zeta potential of Cu_2O@CuO and Cu@Cu_2S

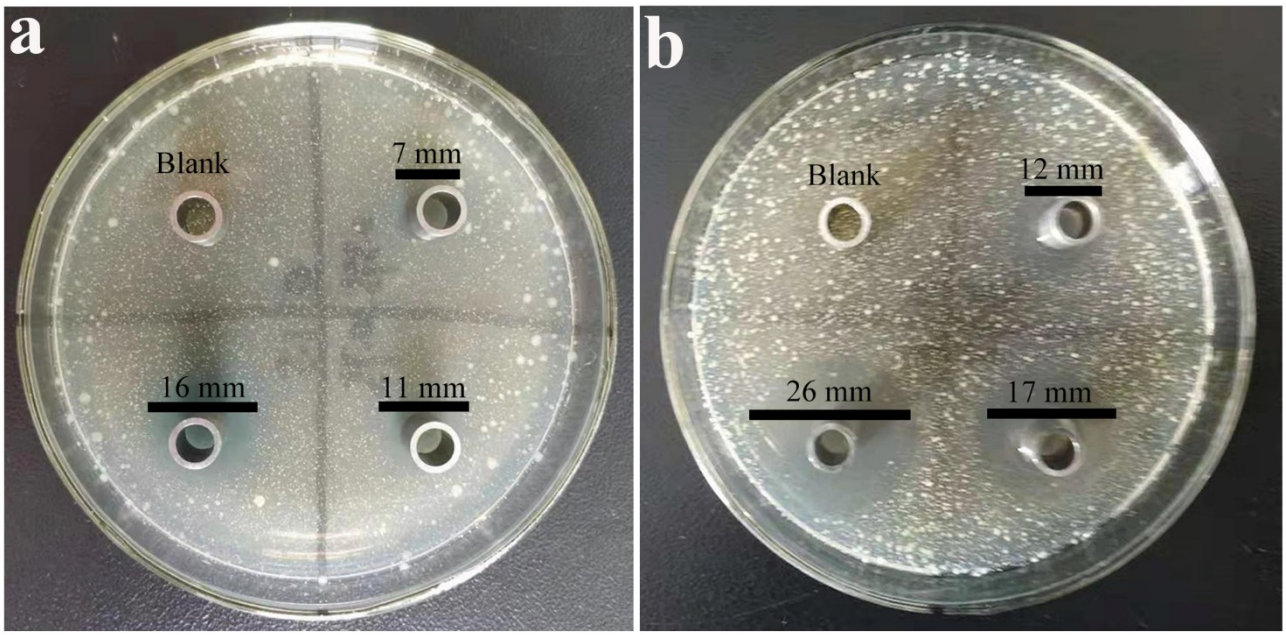

Fig. S20 (a) and (b) Antibacterial zone test against *E. coli* and *S. aureus*

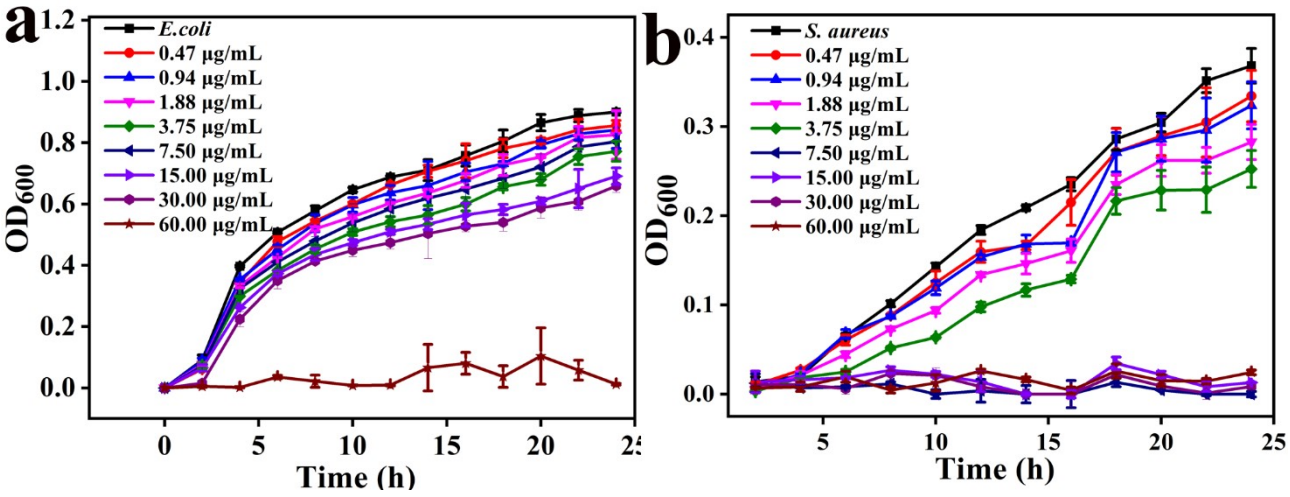

Fig. S21 (a) and (b) Reproduction curves of *E. coli* and *S. aureus* at different concentrations of Cu@Cu_2S nanozymes

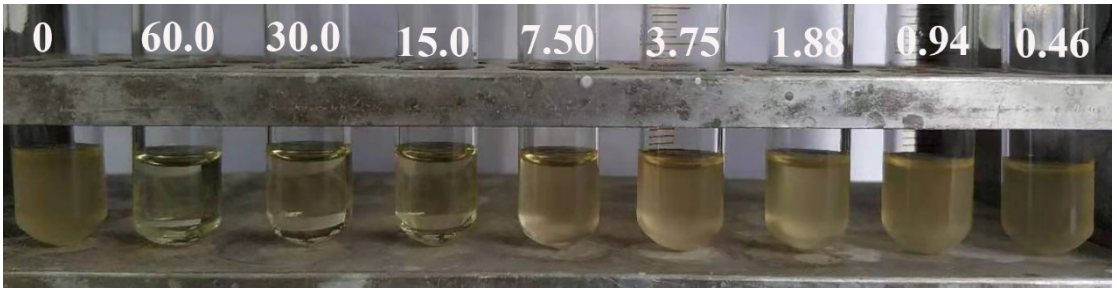

Fig. S22 MICs testing for *S. aureus* with Cu@Cu_2S nanodots in test tubes

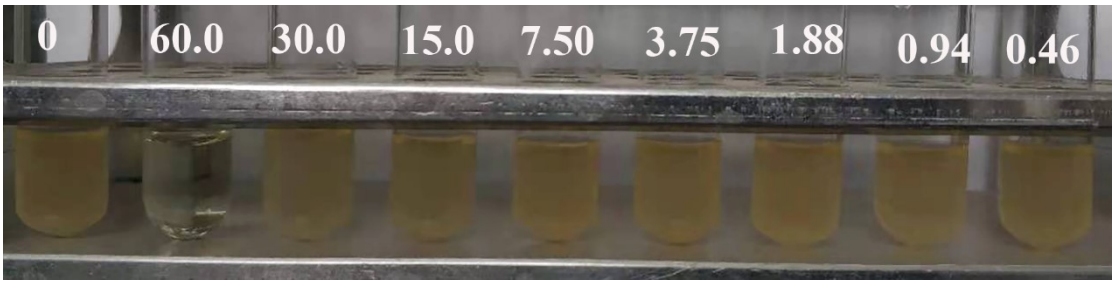

Fig. S23 MIC testing for *E. coli* with Cu@Cu_2S nanodots in test tubes